Simultaneous Occurrence of Quadruple Lewis Acid–Base Interactions between Selenium Atoms in Selenocarbonyl Dimers

Gabriel J. Buralli,[a, b] Darío J. R. Duarte,*[a, b] Nélida M. Peruchena,*[a, b] and Ibon Alkorta[c]

High-level quantum chemical calculations are performed to investigate C=Se···Se=C interactions. Bounded structures are found with binding energies between −4 and −7 kJ mol^{-1}. An energy decomposition analysis shows that dispersion is the more attractive term, and in all cases save one, the electrostatic interaction is attractive despite each selenium atom having a positive σ hole at the extension of the C=Se bond. The topological analysis of the molecular electrostatic potential and $L(\mathbf{r}) = -\nabla^2\rho(\mathbf{r})$ function, and natural bond orbital analysis reveal that these particular Se···Se contacts can be considered to be quadruple Lewis acid–base interactions.

1. Introduction

■■Please give academic titles for all authors■■Chalcogen bonds (YBs) are noncovalent interactions between a chalcogen atom (O, S, Se, Te) and a Lewis base. Several types of these interactions have been reported. Structural, topological, and energetic characteristics are very similar to those of interactions categorized as σ-hole bonding.[1–6]

A recent search of the Cambridge Structural Database (CSD) showed that S···S contacts between cysteine fragments (RCH$_2$SH) prefer parallel orientations. Calculations at the CCSD(T)/CBS level of theory show that this geometry has an interaction energy of −7.5 kJ mol^{-1}.[4] Moreover, selenium is an essential micronutrient that is incorporated as selenocysteine at the active sites of a wide range of proteins.[7] Thus, the control of Se···Se contacts could be of fundamental importance to human health.

A detailed analysis of several YBs reveals that the hybridization of the chalcogen atom can play an important role in their strength. When the chalcogen atom has sp^3 hybridization, the YB is mainly governed by electrostatic and exchange components with less contribution from the dispersive component.[2, 5, 8–10] When the chalcogen atom has sp^2 hybridization, dispersive forces can dominate over electrostatic forces.[1, 11] In other cases, such as F$_2$CSe···NH$_3$, OCS···Cl$^-$, SCS···Cl$^-$, and F$_2$CS···Cl$^-$, YBs are dominated by electrostatic forces and electron charge transfer from the lone pairs of the Lewis base to an antibonding orbital of the Lewis acid.[1, 12] The weak molecular interactions of O=C=S, S=C=S, F$_2$C=S, and Cl$_2$C=S with singlet carbene have studied by Zhao et al., who used a fragment-based energy decomposition analysis (EDA) for the interaction energies to show that that the electrostatic component is the main stabilizing factor in these complexes.[13]

Guo et al.[11, 12] showed through analysis of the molecular electrostatic potential (MEP) that the selenium atom of the F$_2$C=Se molecule can act as Lewis acid and Lewis base. They found that the Se atom has an σ hole (77.9 kJ mol^{-1}) centered around the extension of the C=Se bond and two regions of negative electrostatic potential (−40.8 kJ mol^{-1}) on the two sides of the C=Se bond in the molecular plane, corresponding to the lone pairs on the Se atom. According to these authors, F$_2$C=Se can form YB complexes through the σ hole with N$_2$, NH$_3$, NCH, NHCH$_2$, NMe$_3$, and NCLi, and can act as a Lewis base through the MEP minima and form hydrogen bonds with HX (X = F, Cl, OH, CN) molecules, halogen bonds with dihalogen molecules (BrCl, ClF, and BrF), and dative bonds with BeH$_2$ and BH$_3$.[11, 12]

On the other hand, recently chalcogen···chalcogen contacts[14] have been divided into two categories, depending on their geometry: types I and II (see Scheme 1), like halogen···halogen contacts.[15] According to an extensive crystallographic and theoretical analysis performed by Shukla and Chopra, the C=S···S=C contacts are of dispersive nature with electrostatics contributing to the destabilization in some cases.[14] Even though more than 70% of structures have type I S···S contacts, there are some indications of linear C=S···S=C contacts that were not classified (see Figure 3 f in ref. [14]).

[a] G. J. Buralli, D. J. R. Duarte, N. M. Peruchena
Laboratorio de Estructura Molecular y Propiedades
Área de Química Física, Departamento de Química
Facultad de Ciencias Exactas y Naturales y Agrimensura
Universidad Nacional del Nordeste
Avenida Libertad 5460 (3400) Corrientes (Argentina)
E-mail: djr_duarte@hotmail.com

[b] G. J. Buralli, D. J. R. Duarte, N. M. Peruchena
IQUIBA-NEA (UNNE-CONICET)
Avenida Libertad 5460 (3400) Corrientes (Argentina)
E-mail: arabeshai@yahoo.com.ar

[c] I. Alkorta
Instituto de Química Médica, CSIC
Juan de la Cierva, 3, 28006 Madrid (Spain)

Supporting Information and the ORCID identification number(s) for the author(s) of this article can be found under:
https://doi.org/10.1002/cphc.201700682.

These are not the final page numbers! ↗↗
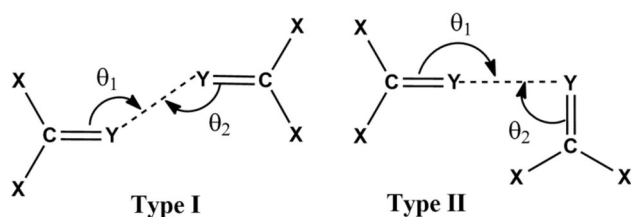
Scheme 1. Schematic representation of chalcogen···chalcogen contacts. Type I: $\theta_1 \cong \theta_2$ and type II, $\theta_1 \cong 180°$, $\theta_2 \cong 90°$.

Most of the characteristics of YBs are understood in terms of the σ-hole concept. However, in several examples in the literature it is shown that the σ-hole concept fails.[16–18] Recently, many of the characteristics of some molecular interactions, such as beryllium bond,[19] pnicogen bonds,[20,21] chalcogen bond,[3,6] halogen bond,[22,23] and O···X (X = O, N) interactions,[24] have been explained through the hole–lump concept,[25,26] extracted from the topology of the $L(\mathbf{r}) = -\nabla^2 \rho(\mathbf{r})$ function. According to this concept, a molecular interaction involving a Lewis acid–base interaction is due to a lump–hole interaction, whereby the full quantum electrostatic potential is used.[20]

The electron density and MEP[27–29] are observable properties of the system that can be experimentally and theoretically studied. In the framework of halogen bonds, we have used the hole–lump concept to explain the simultaneous occurrence of Lewis acid–base interactions in halogen···halogen contacts of types I[30] and II.[23] According to the MEP, it appears that the $R_2C\text{=}Se$ molecules cannot form dimers or binary complexes by facing each other through positive σ holes.[11,12] However, in the present work we found stable linear C=Se···Se=C contacts in which each Se atom simultaneously acts as Lewis acid and base; a similar situation has been already described for pnicogen-bonded dimers.[31–33] This study points out the importance of molecular interactions in which selenocarbonyl groups can participate, and may be useful for recognizing attractive Se···Se contacts in crystal structures and biomolecules.

Computational Details

The geometries of monomers and complexes were optimized by second-order Møller–Plesset perturbation theory (MP2)[34] with the aug-cc-pVTZ basis set. For the Se atom the aug-cc-pVTZ-PP basis set was used. Frequency calculations were performed at the same level of theory. All optimization, harmonic vibrational frequency, and single-point energy calculations at the HF, MP2, and CCSD(T) levels of theory were performed with the Gaussian 09 program package.[35]

The interaction energy was calculated by using the extrapolation scheme proposed by Helgaker et al. [Eqs. (1)–(5)][36,37] following the recommendations of Hobza et al. [Eq. (6)]:[38]

$$E_X^{HF} = E_{CBS}^{HF} + Be^{-X\alpha} \tag{1}$$

$$E_{CBS}^{HF} = \frac{E_4^{HF} e^{4\alpha} - E_3^{HF} e^{3\alpha}}{e^{4\alpha} - e^{3\alpha}} \tag{2}$$

$$E_{coor,X}^{MP2} = E_X^{MP2} - E_X^{HF} \tag{3}$$

$$E_{coor,lim}^{MP2} = \frac{4^3 E_{coor,4}^{MP2} - 3^3 E_{coor,3}^{MP2}}{4^3 - 3^3} \tag{4}$$

$$E_{CBS}^{MP2} = E_{CBS}^{HF} + E_{coor,lim}^{MP2} \tag{5}$$

$$E_{CBS}^{CCSD(T)} = E_{CBS}^{MP2} + \left(E_3^{CCSD(T)2} - E_3^{MP2} \right) \tag{6}$$

where $\alpha = 1.54$ and X is the cardinal number of the employed basis set: 3 for aug-cc-pVTZ (aug-cc-pVTZ-PP for Se) and 4 for aug-cc-pVQZ (aug-cc-pVQZ-PP for Se), and CBS denotes complete basis set.

All complexes were optimized with C_{2v} or D_{2d} symmetry as appropriate. If the symmetry is not imposed, type I or II Se···Se contacts are obtained with similar interaction energies (e.g., for $H_2CSe\cdots SeCH_2$ complexes: type I: -4.2 kJ mol^{-1}, type II: -6.5 kJ mol^{-1}, and type III: -5.2 kJ mol^{-1}, calculated at the CCSD(T)/CBS level of theory).

The interaction energies E_{int} were decomposed by following the localized molecular orbital energy decomposition analysis (LMOEDA)[39] formalism according to Equation (7):

$$E_{int} = E_{elect} + E_{ex\text{-}rep} + E_{pol} + E_{disp} \tag{7}$$

where E_{elect} is the electrostatic term describing the classical Coulomb interaction, $E_{ex\text{-}rep}$ the exchange-repulsion component resulting from the Pauli exclusion principle, and E_{pol} and E_{disp} are polarization and dispersion terms, respectively. These calculations were carried out with the quantum chemistry program package GAMESS (version 2013-R1)[40] at the same level of theory as the optimization.

The intermolecular distributions of the electron density and $L(\mathbf{r}) = -\nabla^2 \rho(\mathbf{r})$ function were studied in the framework of the quantum theory of atoms in molecules (QTAIM)[25,26,41] with the AIMAll program.[42] The molecular electrostatic potential $V(\mathbf{r})$ and electric field lines were calculated with the Multiwfn program.[43] The electron-density shift map was generated as the difference between the electron density of the complex and the sum of the electron densities of the isolated monomers.

To better understand the charge transfer between the monomers, a natural bond orbital (NBO) analysis was carried out at the HF/aug-cc-pVTZ level of theory with MP2/aug-cc-pVTZ geometries.

The maps of the MEP, the envelope of $L(\mathbf{r})$ function and electron-density shifts, and contour lines of the electric field were drawn with JMOL,[44] AIMAll,[42] and Multiwfn[43] programs, respectively.

2. Results and Discussion

The isolated $X_2C\text{=}Se$ (X = H, F, Cl, Br, OH, CH$_3$) molecules show C_{2v} symmetry. The MEP of these molecules shows a σ hole in the extension of the C=Se bond (Figure 1). The electrostatic potentials at the σ hole range between 84.0 and 3.4 kJ mol^{-1} for F$_2$CSe and (CH$_3$)$_2$CSe, respectively (see Table S1 of the Supporting Information).

Selected geometric parameters calculated at the same level of optimization and the interaction energies of $X_2C\text{=}Se\cdots Se\text{=}CY_2$ complexes are reported in Table 1. The interaction energies are similar to those of the YB complexes O=C=S···CH$_2$ (-7.9 kJ mol^{-1}), S=C=S···CH$_2$ (-6.8 kJ mol^{-1}), F$_2$C=S···CH$_2$
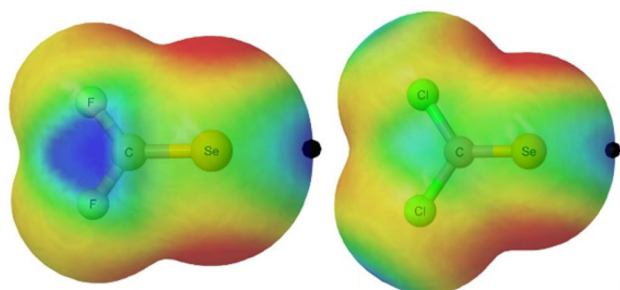
↖↖ These are not the final page numbers!

Figure 1. Electrostatic potential on the 0.001 au electron-density isosurface. The color code is red = −26.2 kJ mol^{-1} and blue = +78.8 kJ mol^{-1}. The location of the σ hole is indicated by a black dot.

Figure 2. Minimum-energy path for the approach of Se atoms of $F_2C=$Se⋯Se$=CF_2$ in linear C=Se⋯Se=C conformation, calculated at the MP2/aug-cc-pVTZ level of theory.

Table 1. Selected geometric parameters and interaction energies.			
Complex	d(Se⋯Se)	Δd(Se⋯Se)[b]	E_{int}[c]
H_2CSe⋯SeCH$_2$	3.385	0.515	−5.1
F_2CSe⋯SeCH$_2$	3.415	0.485	−5.2
Cl_2CSe⋯SeCH$_2$	3.414	0.486	−6.5
Br_2CSe⋯SeCH$_2$	3.393	0.507	−7.1
$(OH)_2$CSe⋯SeCH$_2$	3.411	0.489	−4.1
$(CH_3)_2$CSe⋯SeCH$_2$	3.432	0.468	−5.7
F_2CSe⋯SeCF$_2$	3.508	0.392	−4.3
Cl_2CSe⋯SeCCl$_2$	3.409	0.491	−6.2
Br_2CSe⋯SeCBr$_2$	3.315	0.585	−7.3
$(OH)_2$CSe⋯SeC(OH)$_2$	3.491	0.409	−5.2
$(CH_3)_2$CSe⋯SeC(CH$_3$)$_2$	3.436	0.464	−5.2

[a] d(Se⋯Se) [Å]: intermolecular distances. [b] Δd(Se⋯Se) [Å]: difference between the sum of the van der Waals radii[45] of the Se atoms and intermolecular distances in the complex. E_{Int} [kJ mol^{-1}]: interaction energies calculated at the CCSD(T)/CBS level of theory.

(−5.4 kJ mol^{-1}), and $Cl_2C=$S⋯CH$_2$ (−5.4 kJ mol^{-1}) studied by Zhao et al .[13]

With the aim of discussing the electronic effects of the substituents on the stabilization of these complexes, we replaced the H atoms by various groups of different electron-withdrawing/donating capacity. When the H atoms are replaced by halogen atoms, the interaction energies for heterodimer complexes are ranked according to the size of the substituent: H < F < Cl < Br. Thus, it appears that the electronic effect of a substituent is less relevant than its size. However, for homodimer complexes, the interaction energies follow the order F < H < Cl < Br. When we compare the heterodimers with the corresponding homodimers, differences are observed only for F and OH substituents, whereas for the rest of the complexes no significant differences were observed.

All systems were optimized with C_{2v} or D_{2d} symmetry as appropriate, with the two planes formed by the monomers perpendicular to each other. In most of the complexes studied here small imaginary frequencies (< 20i cm^{-1}) are observed, except for the $H_2C=$Se⋯Se$=CH_2$ and $(CH_3)_2C=$Se⋯Se$=C(CH_3)_2$ complexes, which have no imaginary frequencies. In any case, the systems considered have bounding energies and their dissociation profiles, such as that of the $F_2C=$Se⋯Se$=CF_2$ complex shown in Figure 2, show a relatively deep well (−8.3 kJ mol^{-1}
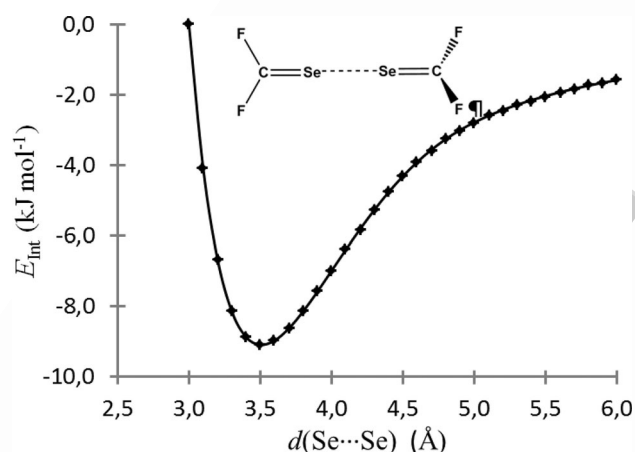
calculated at the MP2/aug-cc-pVTZ level of theory). Similar small imaginary frequencies have been reported for other related systems such as $R_2C=$S⋯Cl$^-$ (R = H, F)[1] and $R_2C=$S⋯CH$_2$ (R = F, Cl)[13] complexes.

These Se⋯Se interactions are of stabilizing nature ($E_{int} < 0$) and range from −4.1 to −7.3 kJ mol^{-1} (see Table 1). These results are in partial agreement with those reported for S⋯S interactions by Shukla and Chopra,[14] according to whom the C=S⋯S=C contacts are stabilizing in some molecular pairs but a consequence of crystal packing in others. In the complexes studied by Shukla and Chopra, the binding energies ranged from −6.7 to +3.7 kJ mol^{-1}.

The C=Se⋯Se=C contacts have intermolecular Se⋯Se distances of about 3.4 Å, which is shorter than the sum of the van der Waals radii (3.9 Å)[45] [Δd(Se⋯Se) > 0 Å]. The two planes that contain the monomers are perpendiculars to each other. This is essentially different to most S⋯S contacts found by Shukla and Chopra.[14] On the basis of this crystallographic study by Shukla et al. and the intermolecular Se⋯Se distances and symmetries of complexes reported herein, it appears that there are three types of chalcogen⋯chalcogen contacts: type I ($\theta_1 \approx \theta_2 \approx$ 140–160°), type II ($\theta_1 \approx$ 180° and $\theta_2 \approx$ 90°), and type III ($\theta_1 \approx \theta_2 \approx$ 180°). However, it appears that only type III $H_2C=$S⋯S$=CH_2$ contacts have been found in crystallographic studies (see Figure 7a in ref. [14]).

Energy decomposition analysis (Table 2) reveals interesting features of C=Se⋯Se=C interactions. In general, the stabilizing electrostatic components E_{elect} and E_{pol} are the least important terms, whereas in all complexes the most important stabilization term is the dispersive component. Moreover, the electrostatic components E_{elect} and E_{pol} are attractive (except for F_2CSe⋯SeCF$_2$, in which $E_{elect} < 0$), although the selenium atoms have a positive σ hole at the extension of C=Se bond. Similar observations have been made for Y⋯Y (Y = O, S, Se, Te) contacts, in which the most important stabilization term is the dispersion.[46] However, these observations are essentially different from those made for the linear F−Br⋯Br−F system,[23] in which the two interacting regions also show positive values of the

These are not the final page numbers! ↗↗

Table 2. Energy decomposition analysis of the interaction energy obtained with the LMOEDA partition scheme.[a]

Complex	E_{elect}	E_{ex-rep}	E_{pol}	E_{disp}	E_{int}
$H_2CSe\cdots SeCH_2$	−5.9	20.4	−4.9	−16.9	−7.2
$F_2CSe\cdots SeCH_2$	−3.7	16.4	−4.3	−15.1	−6.8
$Cl_2CSe\cdots SeCH_2$	−4.3	17.1	−4.6	−16.7	−8.4
$Br_2CSe\cdots SeCH_2$	−4.8	18.5	−4.9	−17.6	−8.8
$(OH)_2CSe\cdots SeCH_2$	−2.5	17.2	−4.6	−17.0	−6.9
$(CH_3)_2CSe\cdots SeCH_2$	−4.1	17.6	−4.2	−17.3	−7.9
$F_2CSe\cdots SeCF_2$	0.5	10.3	−3.1	−13.1	−5.3
$Cl_2CSe\cdots SeCCl_2$	−2.2	16.0	−4.5	−17.5	−8.3
$Br_2CSe\cdots SeCBr_2$	−3.8	22.3	−6.2	−21.1	−8.9
$(OH)_2CSe\cdots SeC(OH)_2$	−0.5	12.3	−2.7	−15.3	−6.5
$(CH_3)_2CSe\cdots SeC(CH_3)_2$	−0.3	13.5	−3.1	−17.4	−7.3

[a] All values in kJ mol^{-1}.

electrostatic potential and the electrostatic component is always repulsive.

Table 3 lists the values of the local topological properties at the Se···Se bond critical points (BCPs) obtained from QTAIM.

Table 3. Local topological properties of the electron density at the Se···Se BCP.[a]

Complex	$\rho(\mathbf{r}_b)$	$\nabla^2\rho(\mathbf{r}_b)$	$H(\mathbf{r}_b)$
$H_2CSe\cdots SeCH_2$	0.0109	0.0349	0.0010
$F_2CSe\cdots SeCH_2$	0.0099	0.0326	0.0011
$Cl_2CSe\cdots SeCH_2$	0.0102	0.0327	0.0010
$Br_2CSe\cdots SeCH_2$	0.0106	0.0339	0.0010
$(OH)_2CSe\cdots SeCH_2$	0.0101	0.0328	0.0011
$(CH_3)_2CSe\cdots SeCH_2$	0.0101	0.0321	0.0010
$F_2CSe\cdots SeCF_2$	0.0079	0.0271	0.0011
$Cl_2CSe\cdots SeCCl_2$	0.0100	0.0324	0.0011
$Br_2CSe\cdots SeCBr_2$	0.0121	0.0380	0.0009
$(OH)_2CSe\cdots SeC(OH)_2$	0.0079	0.0268	0.0011
$(CH_3)_2CSe\cdots SeC(CH_3)_2$	0.0099	0.0317	0.0010

[a] $\rho(\mathbf{r}_b)$: electron density. $\nabla^2\rho(\mathbf{r}_b)$: Laplacian of the electron density. $H(\mathbf{r}_b)$: total electronic energy density.

Figure S1 shows the presence of a BCP and a corresponding bond path that links the interacting Se atoms, and thus confirms that there is a bonding interaction between these atoms. The electron densities, which range from 0.0100 to 0.0121 au, and $\nabla^2\rho(\mathbf{r}_b)$ values, which range from 0.0271 to 0.0380 au, are similar to the values reported for other YB interactions.[11,47] The small and positive values of $\rho(\mathbf{r}_b)$, $\nabla^2\rho(\mathbf{r}_b)$, and $H(\mathbf{r}_b)$ are typical of closed-shell interactions.

The representation of the negative gradient of molecular electrostatic potential $-\nabla V(\mathbf{r})$ [i.e. the electric field $E(\mathbf{r})$] indicates the direction of the Coulombic forces acting on $\mathbf{r}$.[48] Figure 3 a shows the electric field lines (EFLs) of the $H_2CSe\cdots SeCH_2$ complex. Looking at the EFLs at the intermolecular region reveals that the electrostatic forces are directed towards the nuclei of the selenium atoms. Moreover, some of the EFLs that emanate from the local minima of the topology of $V(\mathbf{r})$ (lone pairs of the Se atoms) and head towards the nucleus of the other selenium atom [$V_{S,min}$(Se2)→Nucleus(Se1)]. According to QTAIM the atomic basins of the selenium atoms are divided by a interatomic surface (IAS), indicated by a solid black line in Figure 3 a. The topology of $V(\mathbf{r})$ shows that the basin of Se2 is completely enclosed by a zero-flux surface and the EFLs indicate that there are two regions of high electron density belonging to the Se2 atom that feel the attraction of the nucleus of the other selenium atom (Se1). These regions are defined as the electrostatic attraction region.[49] Due to the symmetry of the system, all previous discussion is valid for the plane perpendicular to that in Figure 3 a, but in the opposite direction. In other words, the two lone pairs of a selenium atom feel the attraction of the nucleus of the other selenium atom and vice versa.

The $L(\mathbf{r})$ function is a powerful tool for the study of acid–base interactions, especially when the electrostatic component plays a minor role.[20] Figure 3 b shows the envelope graph at $L(\mathbf{r}) = 0$ au for the $H_2CSe\cdots SeCH_2$ complex. The regions with high electronic charge concentration [lump-$L(\mathbf{r}) > 0$] of the Se atoms are in orthogonal planes. In this way, four hole–lump interactions overcome the unfavorable lump–lump and hole–

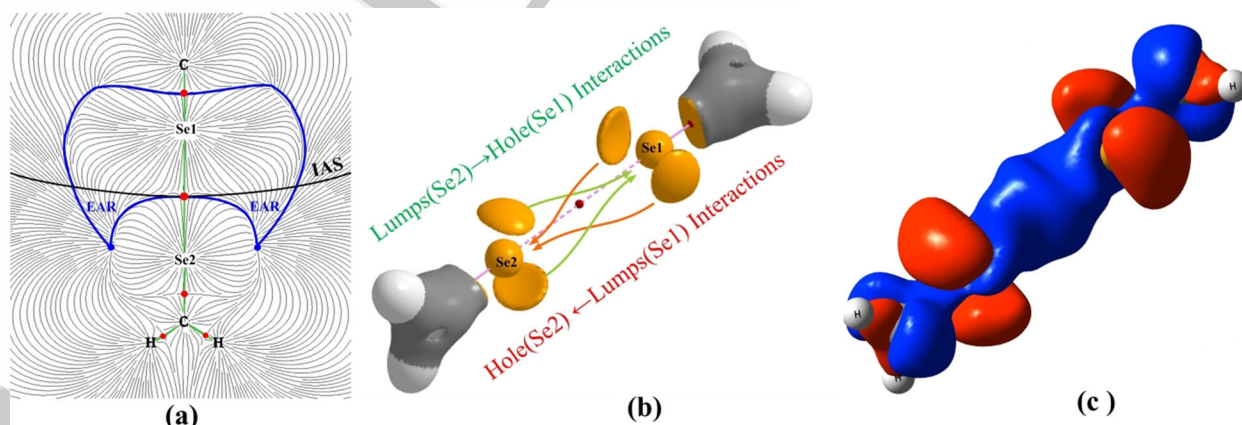**Figure 3.** a) EFLs in the plane of a H2CSe molecule of the $H_2CSe\cdots SeCH_2$ complex. The bond critical points of $V(r)$ are shown (red dots). b) Envelope at $L(r) = 0$ au. Note that the molecules are oriented so that the hole in the valence-shell charge concentration (VSCC) of a selenium atom is aligned with the hole in the VSCC of the other selenium atom. c) Electron density shifts for $H_2CSe\cdots SeCH_2$ complex at the ± 0.0001 au isosurface. Red and blue regions indicate decreased and increased electron densities, respectively.

↖↖ **These are not the final page numbers!**

hole interactions. It appears that multiple hole–lump interactions are the driving forces of type III Se···Se contacts. These multiple simultaneous interactions are consistent with earlier studies performed on other molecular interactions.[20,30,31]

The electron-density shifts that accompany formation of the H_2CSe···$SeCH_2$ complex were calculated, and the results are illustrated in Figure 3c. Blue regions represent the accumulation of additional electron density as a result of the formation of the complex, and red regions indicate loss of electron density. An increment of the electron density in the intermolecular region (blue surface) and a decrease on the lone pairs of the Se atoms (red surface) are observed. In other words, the lone pairs of each Se atoms transfer charge to the intermolecular region, which is attracted by both selenium nuclei. It is logical to assume that the transferred electron density is channeled through the EFL. This is probably the main reason why transferred electronic charge of the lone pairs from each Se atom is mainly accumulated in the intermolecular region.

Normally, the charge transfer is attributed to interaction between the molecular orbitals corresponding to the lone pair of an heteroatom and the antibonding orbitals involving the atom with the σ hole.[50] However, the boundary between polarization (intrinsic component of the electrostatic interaction) and charge transfer is not well defined.[50–53]

Selected donor–acceptor orbital interactions and their second-order perturbation energies calculated by the NBO method are reported in Table 4. In complexes with D_{2d} symmetry only the charge transfer from monomer-1 toward monomer-2 is presented, since in these systems the LP(1)Se1→σ*(C−Se2) and LP(2)Se1→π*(C−Se2) interactions are equivalent to LP(1)Se2→σ*(C−Se1) and LP(2)Se2→π*(C−Se1), respectively. NBO analysis shows that charge transfer occurs in both directions, from the two lone pairs of a selenium atom to the antibonding orbitals of the other monomers and vice versa. In addition, electron transfer from the LP(1)Se1 to the σ*(C−Se2) orbital is greater than that from the LP(2)Se1 to the π*(C−Se2) orbital. Figure 4 shows simultaneous orbital interactions of the lone pairs of a Se atom with the unoccupied antibonding orbitals of the other monomer. It appears that these orbital overlaps play an important role in determining the geometry of these complexes.
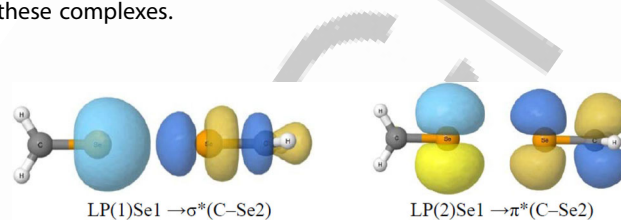

Figure 4. Orbital interactions between occupied and unoccupied antibonding orbitals of the H_2CSe···$SeCH_2$ complex.

On the other hand, systems stabilized mainly by the dispersive forces such as the dimer of methane or noble gas species are usually not classified as Lewis acid–base complexes.[54] However, in these particular Se···Se contacts, in which the main attractive component is dispersion, significant magnitudes of electron transfers are observed. According to Grabowski et al.[54] the electron charge transfer, if it is not negligible, is a signature of Lewis acid–base interactions. It appears to be that in these complexes both monomers simultaneously acts as Lewis acid and base.

3. Conclusions

We have investigated the nature of a particular type of intermolecular interactions established between two selenocarbonyl molecules. Theoretical calculations show that stable complexes with linear structures C=Se···Se=C are formed, although both selenium atoms have a positive σ hole at the extension of the C=Se bond. The LMOEDA scheme reveals that the dispersive forces play a key role in stabilizing these complexes. In addition, it is also observed that the electrostatic components E_{elect} and E_{pol} are stabilizing, although two positive σ holes face one another. The joint analysis of the electric field lines, the $L(\mathbf{r}) = -\nabla^2\rho(\mathbf{r})$ function, electron-density shift, and NBO analysis reveal that these particular Se···Se contacts can be considered to be quadruple Lewis acid–base interactions. Finally, a new class of chalcogen···chalcogen contacts has been reported in this study, which we name type III ($\theta_1 \approx \theta_2 \approx 180°$).

Table 4. NBO analysis for studied complexes, occupation numbers of selected molecular orbitals, and second-order perturbation energies $E^{(2)}$ (donor→acceptor).[a]

Complex	LP(1)Se1→σ*(C−Se2)			LP(2)Se1→π*(C−Se2)		
	LP1	σ*	$E^{(2)}$	LP2	π*	$E^{(2)}$
H_2CSe···$SeCH_2$	1.988	0.006	10.9	1.942	0.004	3.2
F_2CSe···$SeCH_2$	1.981	0.005	8.9	1.888	0.002	2.2
Cl_2CSe···$SeCH_2$	1.971	0.005	8.6	1.887	0.003	2.5
Br_2CSe···$SeCH_2$	1.967	0.005	8.9	1.880	0.003	2.7
$(OH)_2CSe$···$SeCH_2$	1.980	0.005	9.4	1.904	0.003	2.8
$(CH_3)_2CSe$···$SeCH_2$	1.974	0.005	8.7	1.943	0.004	3.0
F_2CSe···$SeCF_2$	1.982	0.025	7.6	1.890	0.161	1.6
Cl_2CSe···$SeCCl_2$	1.972	0.036	8.5	1.888	0.211	3.0
Br_2CSe···$SeCBr_2$	1.966	0.036	11.1	1.880	0.204	3.8
$(OH)_2CSe$···$SeC(OH)_2$	1.979	0.029	8.9	1.905	0.292	1.3
$(CH_3)_2CSe$···$SeC(CH_3)_2$	1.974	0.023	9.9	1.943	0.086	2.7
	LP(1)Se2→σ*(C−Se1)			LP(2)Se2→π*(C−Se1)		
	LP1	σ*	E^2	LP2	π*	E^2
F_2CSe···$SeCH_2$	1.989	0.027	10.9	1.944	0.159	2.6
Cl_2CSe···$SeCH_2$	1.989	0.036	9.3	1.944	0.208	3.2
Br_2CSe···$SeCH_2$	1.989	0.036	9.9	1.943	0.202	3,1
$(OH)_2CSe$···$SeCH_2$	1.988	0.023	11.3	1.943	0.235	2.2
$(CH_3)_2CSe$···$SeCH_2$	1.989	0.023	10.5	1.943	0.087	2.5

[a] Energies in kJ mol^{-1} and occupation numbers in electrons.

Conflict of interest

The authors declare no conflict of interest.

[1] W. Wang, B. Ji, Y. Zhang, *J. Phys. Chem. A* **2009**, *113*, 8132–8135.

[2] U. Adhikari, S. Scheiner, *J. Phys. Chem. A* **2014**, *118*, 3183–3192.

[3] E. Alikhani, F. Fuster, B. Madebene, S. J. Grabowski, *Phys. Chem. Chem. Phys.* **2014**, *16*, 2430–2442.

[4] I. S. Antonijević, G. V. Janjić, M. K. Milčić, S. D. Zarić, *Cryst. Growth Des.* **2016**, *16*, 632–639.

[5] L. M. Azofra, I. Alkorta, S. Scheiner, *Theor. Chem. Acc.* **2014**, *133*, 1586.

[6] M. E. Brezgunova, J. Lieffrig, E. Aubert, S. Dahaoui, P. Fertey, S. Lebègue, J. G. Ángyán, M. Fourmigué, E. Espinosa, *Cryst. Growth Des.* **2013**, *13*, 3283–3289.

[7] K. M. Brown, J. R. Arthur, *Public Health Nutr.* **2001**, *4*, 593–599.

[8] U. Adhikari, S. Scheiner, *Chem. Phys. Lett.* **2011**, *514*, 36–39.

[9] R. Shukla, D. Chopra, *J. Phys. Chem. B* **2015**, *119*, 14857–14870.

[10] R. Shukla, D. Chopra, *J. Chem. Sci.* **2016**, *128*, 1589–1596.

[11] X. Guo, X. An, Q. Li, *J. Phys. Chem. A* **2015**, *119*, 3518–3527.

[12] X. Guo, Q. Li, *J. Mol. Model.* **2015**, *21*, 157.

[13] Q. Zhao, D. Feng, Y. Sun, J. Hao, Z. Cai, *Int. J. Quantum Chem.* **2011**, *111*, 3881–3887.

[14] R. Shukla, D. Chopra, *Cryst. Growth Des.* **2016**, *16*, 6734–6742.

[15] N. Ramasubbu, R. Parthasarathy, P. Murray-Rust, *J. Am. Chem. Soc.* **1986**, *108*, 4308–4314.

[16] Y. Zhang, N. Ma, W. Wang, *Chem. Phys. Lett.* **2012**, *532*, 27–30.

[17] K. E. Riley, P. Hobza, *J. Chem. Theory Comput.* **2008**, *4*, 232–242.

[18] J. S. Murray, P. Lane, P. Politzer, *Int. J. Quantum Chem.* **2007**, *107*, 2286–2292.

[19] K. Eskandari, *J. Mol. Model.* **2012**, *18*, 3481–3487.

[20] K. Eskandari, N. Mahmoodabadi, *J. Phys. Chem. A* **2013**, *117*, 13018–13024.

[21] I. Alkorta, J. Elguero, J. E. Del Bene, *J. Phys. Chem. A* **2013**, *117*, 4981–4987.

[22] K. Eskandari, H. Zariny, *Chem. Phys. Lett.* **2010**, *492*, 9–13.

[23] D. J. R. Duarte, G. L. Sosa, N. M. Peruchena, I. Alkorta, *Phys. Chem. Chem. Phys.* **2016**, *18*, 7300–7309.

[24] D. J. R. Duarte, M. S. Miranda, J. C. G. E. da Silva, J. F. Liebman, *Struct. Chem.* **2016**, *27*, 1743–1751.

[25] R. F. W. Bader, *Atoms in Molecules. A Quantum Theory*, Clarendon, Oxford, **1990**.

[26] P. L. A. Popelier, *Atoms in Molecules. An Introduction*, Prentice-Hall, Manchester, **2000**.

[27] *Chemical Applications of Atomic and Molecular Electrostatic Potentials* (Eds.: P. Politzer, D. Truhlar), Plenum Press, New York, **1981**.

[28] P. Politzer, J. S. Murray, T. Clark, *Phys. Chem. Chem. Phys.* **2013**, *15*, 11178–11189.

[29] G. Naray-Szabo, G. G. Ferenczy, *Chem. Rev.* **1995**, *95*, 829–847.

[30] D. J. R. Duarte, N. M. Peruchena, I. Alkorta, *J. Phys. Chem. A* **2015**, *119*, 3746–3752.

[31] J. E. Del Bene, I. Alkorta, G. Sanchez-Sanz, J. Elguero, *Chem. Phys. Lett.* **2011**, *512*, 184–187.

[32] J. E. Del Bene, G. Sanchez-Sanz, I. Alkorta, J. Elguero, *Chem. Phys. Lett.* **2012**, *538*, 14–18.

[33] J. E. Del Bene, I. Alkorta, G. Sanchez-Sanz, J. Elguero, *J. Phys. Chem. A* **2012**, *116*, 3056–3060.

[34] C. Møller, M. S. Plesset, *Phys. Rev.* **1934**, *46*, 618–622.

[35] Gaussian 09 (Revision A.01), M. J. Frisch, G. W. Trucks, H. B. Schlegel, G. E. Scuseria, M. A. Robb, J. R. Cheeseman, G. Scalmani, V. Barone, B. Mennucci, G. A. Petersson, H. Nakatsuji, M. Caricato, X. Li, H. P. Hratchian, A. F. Izmaylov, J. Bloino, G. Zheng, J. L. Sonnenberg, M. Hada, M. Ehara, K. Toyota, R. Fukuda, J. Hasegawa, M. Ishida, T. Nakajima, Y. Honda, O. Kitao, H. Nakai, T. Vreven, J. A. Montgomery, Jr., J. E. Peralta, F. Ogliaro, M. Bearpark, J. J. Heyd, E. Brothers, K. N. Kudin, V. N. Staroverov, R. Kobayashi, J. Normand, K. Raghavachari, A. Rendell, J. C. Burant, S. S. Iyengar, J. Tomasi, M. Cossi, N. Rega, J. M. Millam, M. Klene, J. E. Knox, J. B. Cross, V. Bakken, C. Adamo, J. Jaramillo, R. Gomperts, R. E. Stratmann, O. Yazyev, A. J. Austin, R. Cammi, C. Pomelli, J. W. Ochterski, R. L. Martin, K. Morokuma, V. G. Zakrzewski, G. A. Voth, P. Salvador, J. J. Dannenberg, S. Dapprich, A. D. Daniels, O. Farkas, J. B. Foresman, J. V. Ortiz, J. Cioslowski, D. J. Fox, Gaussian, Inc., Wallingford, CT, **2009**.

[36] A. Halkier, T. Helgaker, P. Jørgensen, W. Klopper, J. Olsen, *Chem. Phys. Lett.* **1999**, *302*, 437–446.

[37] A. Halkier, W. Klopper, T. Helgaker, P. Jørgensen, P. R. Taylor, *J. Chem. Phys.* **1999**, *111*, 9157–9167.

[38] P. Jurecka, J. Sponer, J. Cerný, P. Hobza, *Phys. Chem. Chem. Phys.* **2006**, *8*, 1985–1993.

[39] P. Su, H. Li, *J. Chem. Phys.* **2009**, *131*, 014102.

[40] M. W. Schmidt, K. K. Baldridge, J. A. Boatz, S. T. Elbert, M. S. Gordon, J. H. Jensen, S. Koseki, N. Matsunaga, K. A. Nguyen, S. Su, T. L. Windus, M. Dupuis, J. A. Montgomery, *J. Comput. Chem.* **1993**, *14*, 1347–1363.

[41] R. J. Matta, C. F. Boyd, *The Quantum Theory of Atoms in Molecules: From Solid State to DNA and Drug Design*, Wiley-VCH, Weinheim, **2007**.

[42] T. A. Keith, AIMAll (Version 11.12.19); TK Gristmill Software, Overland Park KS, **2011**; http://aim.tkgristmill.com.

[43] T. Lu, F. Chen, *J. Comput. Chem.* **2012**, *33*, 580–592.

[44] J. (Version 14. 4), an open-source J. viewer for chemical structures in 3D. http://www.jmol.org/.

[45] A. Bondi, *J. Phys. Chem.* **1964**, *68*, 441–451.

[46] C. Bleiholder, D. B. Werz, H. Köppel, R. Gleiter, *J. Am. Chem. Soc.* **2006**, *128*, 2666–2674.

[47] M. D. Esrafili, F. Mohammadian-Sabet, *J. Mol. Model.* **2015**, *21*, 65.

[48] N. Bouhmaida, M. Dutheil, N. E. Ghermani, P. Becker, *J. Chem. Phys.* **2002**, *116*, 6196–6204.

[49] I. Mata, E. Molins, I. Alkorta, E. Espinosa, *J. Phys. Chem. A* **2015**, *119*, 183–194.

[50] A. E. Reed, L. A. Curtiss, F. Weinhold, *Chem. Rev.* **1988**, *88*, 899–926.

[51] M. J. S. Phipps, T. Fox, C. S. Tautermann, C.-K. Skylaris, *Chem. Soc. Rev.* **2015**, *44*, 3177–3211.

[52] W. A. Sokalski, S. M. Roszak, *J. Mol. Struct. THEOCHEM* **1991**, *234*, 387–400.

[53] J. Chen, T. J. Martínez, *Chem. Phys. Lett.* **2007**, *438*, 315–320.

[54] *Practical Aspects of Computational Chemistry IV* (Eds.: J. Leszczynski, M. K. Shukla), New York, **2016**.■■publisher missing?■■

↖↖ **These are not the final page numbers!**

ARTICLES

Se⋯Se contacts of a third kind: An ab initio study on intermolecular interactions between two selenocarbonyl molecules shows that stable complexes with linear structures are formed, although both Se atoms have a positive σ hole at the extension of the C=Se bond (see figure). A class of chalcogen⋯chalcogen contact—denoted type III—is presented.

σ-hole⋯σ-hole interaction?
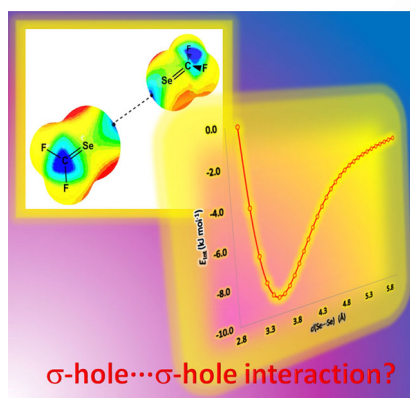
G. J. Buralli, D. J. R. Duarte,*
N. M. Peruchena,* I. Alkorta

■■ – ■■

Simultaneous Occurrence of Quadruple Lewis Acid–Base Interactions between Selenium Atoms in Selenocarbonyl Dimers

Type-III #selenium-selenium #noncovalent interactions presented @unneargentina SPACE RESERVED FOR IMAGE AND LINK

Share your work on social media! *ChemPhysChem* has added Twitter as a means to promote your article. Twitter is an online microblogging service that enables its users to send and read text-based messages of up to 140 characters, known as "tweets". Please check the pre-written tweet in the galley proofs for accuracy. Should you or your institute have a Twitter account, please let us know the appropriate username (i.e., @accountname), and we will do our best to include this information in the tweet. This tweet will be posted to the journal's Twitter account @ChemPhysChem (follow us!) upon online publication of your article, and we recommended you to repost ("retweet") it to alert other researchers about your publication.

Please check that the ORCID identifiers listed below are correct. We encourage all authors to provide an ORCID identifier for each coauthor. ORCID is a registry that provides researchers with a unique digital identifier. Some funding agencies recommend or even require the inclusion of ORCID IDs in all published articles, and authors should consult their funding agency guidelines for details. Registration is easy and free; for further information, see http://orcid.org/.

Gabriel J. Buralli
Darío J. R. Duarte http://orcid.org/0000-0003-2353-3320
Nélida M. Peruchena
Ibon Alkorta

These are not the final page numbers! ↗↗